HHS Public Access

Author manuscript

Mol Microbiol. Author manuscript; available in PMC 2020 March 01.

Published in final edited form as:

Mol Microbiol. 2019 March ; 111(3): 811–824. doi:10.1111/mmi.14193.

LiaR-Independent Pathways to Daptomycin Resistance in *Enterococcus faecalis* Reveal A Multilayer Defense Against Cell Envelope Antibiotics

William R. Miller[1,2,#], **Truc T. Tran**[1,2], **Lorena Diaz**[1,5], **Rafael Rios**[5], **Ayesha Khan**[1,3], **Jinnethe Reyes**[1,5], **Amy G. Prater**[6], **Diana Panesso**[1,2,5], **Yousif Shamoo**[6], and **Cesar A. Arias**[1,2,3,4,5]

[1]Center for Antimicrobial Resistance and Microbial Genomics, University of Texas Health Science Center, McGovern School of Medicine, Houston, TX, USA

[2]Division of Infectious Diseases, University of Texas Health Science Center, McGovern School of Medicine, Houston, TX, USA

[3]Department of Microbiology and Molecular Genetics, University of Texas Health Science Center, McGovern School of Medicine, Houston, TX, USA

[4]Center for Infectious Diseases, University of Texas Health Science Center, School of Public Health, Houston, TX, USA

[5]Molecular Genetics and Antimicrobial Resistance Unit, International Center for Microbial Genomics, Universidad El Bosque, Bogotá, Colombia

[6]Department of BioSciences, Rice University, Houston, TX, USA

Summary

The lipopeptide antibiotic daptomycin (DAP) is a key drug against serious enterococcal infections, but emergence of resistance in the clinical setting is a major concern. The LiaFSR system plays a prominent role in the development of DAP resistance (DAP-R) in enterococci, and blocking this stress response system has been proposed as a novel therapeutic strategy. In this work, we identify LiaR-independent pathways in *E. faecalis* that regulate cell membrane adaptation in response to antibiotics. We adapted *E. faecalis* OG1RF (a laboratory strain) and S613TM (a clinical strain) lacking *liaR* to increasing concentrations of DAP, leading to the development of DAP-R and elevated MICs to bacitracin and ceftriaxone. Whole genome sequencing identified changes in the YxdJK two-component regulatory system and a putative fatty acid kinase (*dak*) in both DAP-R strains. Deletion of the gene encoding the YxdJ response regulator in both the DAP-R mutant and wild type OG1RF decreased MICs to DAP, even when a functional LiaFSR system was present. Mutations in *dak* were associated with slower growth, decreased membrane fluidity and alterations of cell morphology. These findings suggest overlapping stress response pathways can provide protection against antimicrobial peptides in *E. faecalis* at a significant cost in bacterial fitness.

[#] Address correspondence to William R. Miller, William.R.Miller@uth.tmc.edu, Phone: 713-500-6760.

Author Contributions

WRM, YS, and CAA contributed to the conception and design of the study. WRM, TT, LD, RR, AK, JR, AGP and DP contributed to the analysis and acquisition of data, including generation of mutants, preparation and analysis of strains for WGS, electron and fluorescent microscopy, and Laurdan GP analysis. WRM, YS and CAA contributed to writing of the manuscript.

Graphical Abstract

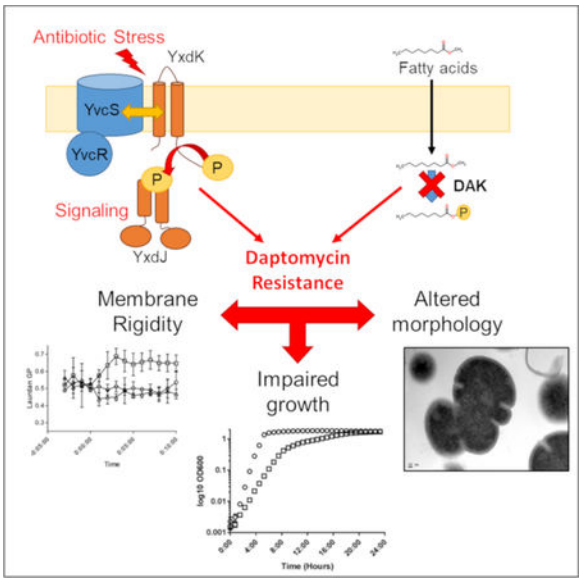

Abbreviated Summary

Resistance to daptomycin, a front line antibiotic for vancomycin-resistant enterococcal infections, is a growing clinical challenge. Through an adaptive evolution experiment, the two component signaling system YxdJK and a putative fatty acid kinase were linked to daptomycin resistance in *Enterococcus faecalis* lacking the primary stress response system LiaFSR. Resistance comes with a cost, as mutants displayed impaired growth with alterations in membrane fluidity, and in some cases distinct alterations of cell morphology.

Keywords

Enterococcus faecalis; antibiotic resistance; daptomycin; stress response; two-component regulatory system; bacterial membrane

Introduction

Enterococci are a leading cause of healthcare-associated infections (Weiner *et al.*, 2016) and treatment is complicated by their resistance to a variety of antimicrobial agents. Indeed, the emergence of resistance to daptomycin (DAP), a lipopeptide antibiotic with dose-dependent bactericidal activity *in vitro* against enterococci, is an example of a pattern of successful adaptations against antimicrobials by these organisms (Arias and Murray, 2012). The mechanism of DAP action is not fully understood but the available evidence suggests that DAP binds to the anionic phospholipid phosphatidylglycerol (PG) in the outer leaflet of the cell membrane in a calcium dependent manner. After initial binding, as more molecules accumulate at the site of action, DAP forms oligomers and appears to transition across the outer to the inner leaflet of the membrane (Tran *et al.*, 2015). The interactions of DAP with the cell membrane alter its structure and function, causing changes in membrane order and

the displacement of membrane-associated proteins responsible for cell envelope biogenesis, ultimately leading to cell death (Müller *et al.*, 2016).

Over 30 genes have been associated with DAP resistance (Arias *et al.*, 2011; Palmer *et al.*, 2011; Humphries *et al.*, 2012; Diaz *et al.*, 2014) in clinical and laboratory isolates of enterococci. A unifying theme associated with the resistance phenotype is the presence of mutations in genes encoding two- or three-component regulatory systems (TCS) and enzymes with predicted roles in phospholipid metabolism. Among the TCS, the LiaFSR system has been shown to play a major role in the maintenance of cell envelope stability under the DAP "attack" (Tran *et al.*, 2013). For example, in an evolutionary model of development of DAP-R in *E. faecalis*, changes in the LiaFSR system occurred first, followed by major increases in the DAP MIC associated with substitutions in cardiolipin synthase (Miller *et al.*, 2013). Similarly, changes in LiaFSR in clinical strains of *E. faecium* led to a loss of DAP bactericidal activity and preceded the emergence of clinical resistance (Munita *et al.*, 2012; Munita *et al.*, 2013). The major role of the LiaFSR system in DAP resistance has been confirmed by targeted deletions of *liaR* (encoding the response regulator of the system) in both *E. faecalis* and *E. faecium*, independent of the genetic background of the strain. These deletions have uniformly led to a DAP "hypersusceptible" phenotype with a decrease in DAP MICs over 100-fold (Panesso *et al.*, 2015; Reyes *et al.*, 2015).

Here, we aimed to discover and characterize new genes associated with the maintenance of cell envelope integrity in *E. faecalis* by adapting strains lacking LiaR to ascending concentrations of DAP. We found that resistance arising independent of LiaR is associated with changes in the TCS YxdJK and in a putative enzyme involved in extracellular lipid metabolism (a dihydroxyacetone kinase-like enzyme, designated DAK). The resistance phenotype was associated with major fitness costs for the cell, suggesting that the redundancy of genetic pathways is hierarchical and alternative pathways for resistance may not be evolutionary advantageous in some contexts.

Results

Emergence of DAP-resistance in the absence of LiaR.

We sought to elucidate whether additional networks can adapt to protect against DAP-triggered membrane damage when the primary mechanism for stress response is no longer available to *E. faecalis*. To test this hypothesis, we exposed both a modified clinical isolate that lacked *liaR* (S613TMΔ*liaR*, a derivative of the clinical isolate S613 harboring the "resistance" alleles $liaF_{\Delta Ile177}$, $gdpD_{\Delta Ile170}$ and $cls_{\Delta Lys61}$) (Reyes *et al.*, 2015), and a laboratory strain OG1RFΔ*liaR* (Supplementary Table 1) to increasing sub-inhibitory concentrations of DAP in an *in vitro* adaptation experiment. The alleles $liaF_{\Delta Ile177}$, $gdpD_{\Delta Ile170}$ and $cls_{\Delta Lys61}$ were previously identified in a DAP-R clinical strain (Arias *et al.*, 2011), and lead to activation of the LiaFSR system (in the case of $liaF_{\Delta Ile177}$) or are predicted to alter membrane phospholipid metabolism ($gdpD_{\Delta Ile170}$ and $cls_{\Delta Lys61}$). After 15 and 17 days, respectively, we selected derivatives of both parent strains in which the MIC had increased to 24 μg/ml (S613TMΔ$liaR_{yvcR219dak84asa1}$) and 6 μg/ml (OG1RFΔ$liaR_{yxdK202dak371ace}$) (Table 1). Unlike prior mutations associated with the LiaFSR pathway, resistance to DAP in the setting of the deletion of *liaR* resulted in a marked fitness

cost, with an increase in the lag phase and longer time to reach stationary phase (Fig. 1, Table 2). This effect was seen in both brain heart infusion (BHI) and Mueller Hinton (MH) media. Since the resistant mutants displayed a small colony variant morphology, we performed colony counts with S613TMΔ*liaR*$_{yvcR219dak84asa1}$ and OG1RFΔ*liaR*$_{yxdK202dak371ace}$ to confirm that OD_{600nm} was proportional to the number of viable bacteria and correlated with spectrophotometer readings (Supplementary Fig. 1). The stability of the resistance phenotype was variable, with the emergence of a heterogeneous population with mixed MICs to DAP in OG1RFΔ*liaR*$_{yxdK202dak371ace}$ after passage in antibiotic free media for 7 days. S613TMΔ*liaR*$_{yvcR219dak84asa1}$ remained resistant (Supplementary Fig. 2). Interestingly, OG1RFΔ*liaR*$_{yxdK202dak371ace}$ also displayed major increases in the MIC to bacitracin (24 fold) and ceftriaxone (>16 fold). Neither derivative displayed major changes in susceptibility to ampicillin or vancomycin (Table 1).

We performed whole genome sequencing of the DAP-R derivatives in both strain backgrounds in order to identify genetic changes associated with development of DAP-R (Table 3). Interestingly, both strains developed mutations in the sensing module of the two-component regulatory system YxdJK, a BceAB-like system previously linked to bacitracin (BAC) resistance in *Bacillus subtilis* and *E. faecalis* and chlorhexidine tolerance in *E. faecium* (Dintner *et al.*, 2014; Gebhard *et al.*, 2014; Prieto *et al.*, 2017). The YxdJK system encodes a sensor histidine kinase (*yxdK*) and cognate response regulator (*yxdJ*), which positively regulates a putative ABC transporter (YvcRS, required for signal transduction along with YxdK) and a second transporter (YxdLM) responsible for the BAC resistance phenotype (Gebhard *et al.*, 2014). Furthermore, both strains were also found to have changes in a gene (*dak*) which encodes a putative enzyme of the dihydroxyacetone kinase (DAK) family whose homolog in *Staphylococcus aureus* has been implicated in the metabolism of extracellular fatty acids (Parsons *et al.*, 2014). Of note, neither gene has been previously associated with DAP-R. Each strain also had predicted substitutions in two major enterococcal virulence factors linked to extracellular matrix adhesion (aggregation substance and a collagen adhesin). We chose to further investigate the roles of the signal transduction system YxdJK and the putative lipid metabolism enzyme DAK in DAP resistance, since previous work has shown that activation of a stress response system coordinated with alteration of lipid metabolism is sufficient for DAP resistance (Miller *et al.*, 2013; Diaz *et al.*, 2014).

The two-component system YxdJK is associated with resistance to cell envelope antibiotics in the absence of a functional LiaFSR system.

Comparison of the antimicrobial susceptibility profiles of OG1RFΔ*liaR* and its DAP-R derivative showed a 24-fold increase in BAC MIC, suggesting that the observed genetic changes resulted in activation of the YxdJK regulatory network, a system previously associated with BAC resistance in *E. faecalis* (Gebhard *et al.*, 2014). No changes were seen in the BAC sensitivities of S613TMΔ*liaR*$_{yvcR219dak84asa1}$, likely due to the fact that this clinical strain also carries the *bcrABDR* operon, a transferable determinant which provides resistance to bacitracin through production of the BcrAB ATP-binding cassette (ABC) transporter and BcrD, an undecaprenol kinase (Manson *et al.*, 2004).

To characterize the contributions of YxdJK to cell envelope active antimicrobials, we constructed a non-polar deletion of the gene encoding the response regulator YxdJ in the DAP resistant OG1RFΔ*liaR*$_{yxdK202dak371ace}$. We postulated that inactivation of the YxdJK system, via deletion of *yxdJ*, would eliminate the adaptive response and lead to significant decreases in the MICs of DAP, BAC and ceftriaxone (CRO). Indeed, loss of *yxdJ* resulted in a 64-fold drop in the MIC of DAP (6 to 0.094 μg/mL) and 128-fold drop in the MIC of BAC (96 to 0.75 μg/mL) confirming the importance of the YxdJK signaling system in resistance to these envelope targeting antimicrobials. Interestingly, we observed no change in the MIC of CRO (Table 1), a finding explained by our investigation of *dak* (see below). Complementation of OG1RFΔ*liaR*$_{yxdK202dak371ace}$Δ*yxdJ* in *trans* using the plasmid pAT392 (Arthur *et al.*, 1994) containing *yxdJ* increased the DAP MIC from 0.094 μg/mL in the deletion mutant to 3 μg/mL in the complemented strain. Complementation also led to an increase in the BAC MIC from 0.75 μg/mL to >256 μg/mL.

Next, we removed the gene encoding YxdJ from wild type OG1RF (OG1RFΔ*yxdJ*) to examine the effect on membrane stress in *E. faecalis* with a functional LiaFSR system. Despite the presence of a functional LiaFSR operon, we observed a 4, 5 and 4-fold decrease in the MICs of DAP, BAC and CRO in the OG1RFΔ*yxdJ* deletion mutant compared to OG1RF, respectively (Table 1). Importantly, this decrease in DAP MIC provides further evidence that the protective effect of YxdJK against the antimicrobial peptide attack is mediated by a LiaFSR-independent mechanism. Introduction of *yxdJ* on plasmid pAT392 (Arthur *et al.*, 1994) (OG1RFΔ*yxdJ*/pAT392::*yxdJ*) restored the MIC of the three above antibiotics to wild type levels, confirming the vital role of the YxdJK system in resistance against cell envelope antibiotics.

Mutations in a gene (*dak*) encoding a putative fatty-acid kinase, augment YxdJK mediated DAP susceptibility and markedly affect cell fitness.

The *dak* gene encodes a 558 amino acid protein with 53% amino acid identity to a fatty acid kinase previously described in *Staphylococcus aureus* (Parsons *et al.*, 2014). This enzyme is capable of phosphorylating exogenous fatty acids for incorporation into membrane phospholipid synthesis. Our analysis identified two substitutions in DAK; the first resulted in a change of serine to proline at position 84 (in S613TMΔ*liaR*$_{yvcR219dak84asa1}$; Table 3), which is predicted to eliminate a hydrogen bond at the ATP binding site of DAK based on comparative modeling using the dihydroxyacetone kinase of *Citrobacter freundii* (Siebold *et al.*, 2003; Kelley *et al.*, 2015). The substitution of a proline into this position is also likely to distort the local main chain resulting in additional changes within the ligand-binding pocket. The second substitution introduces a premature stop codon at position 371 resulting in a truncation of the C-terminal 187 amino acids (in OG1RFΔ*liaR*$_{yxdK202dak371ace}$; Table 3). The predicted changes in the ATP binding site or the loss of the C-terminal end of the protein (containing the K domain involved in substrate phosphorylation) suggested that the enzymatic activity of DAK was likely to be impaired.

In order to confirm the role of DAK in DAP resistance, we complemented the wild type allele encoding the full length protein back into the DAP-R OG1RFΔ*liaR*$_{yxdK202dak371ace}$. The DAP MIC for the complemented strain was reduced from 6 to 2 μg/mL, which is within

the susceptible range. This strain still carries the $YxdK_{A202E}$ amino acid substitution, thus the full resistance phenotype requires both *yxdK* and *dak* mutations to be present. There were no significant changes in the MICs of the other antimicrobials tested, and the DAP MIC remained above that of the OG1RFΔ*liaR* parent strain, likely due to the presence of the mutant *yxdK* allele (Table 1).

We next attempted to produce a deletion mutant of the *dak* gene in OG1RFΔ*liaR*. Our initial attempts to remove the entire reading frame in this strain were unsuccessful. Thus, we designed a strategy to remove the coding region from amino acid 371 to the stop codon at the C-terminal end (OG1RFΔ*liaR*Δ*c-dak*), recapitulating the effect of the frameshift seen in the evolved OG1RFΔ$liaR_{yxdK202dak371ace}$ strain. We observed an increase in the lag phase and a slower growth rate in the OG1RFΔ*liaR*Δ*c-dak* mutant compared to the parental OG1RFΔ*liaR* similar to that of OG1RFΔ$liaR_{yxdK202dak371ace}$ (Fig. 1B, Table 2), suggesting that the change in DAK was likely responsible for the cell fitness effect. Table 1 shows that deletion of the C-terminal end of DAK alone did not have a significant impact on the DAP MIC. In contrast, it increased the ceftriaxone MIC >16 fold without changes in the ampicillin MIC, suggesting that the change influences cephalosporin susceptibility. We complemented the wild type *dak* allele encoding the full-length protein back into the deletion mutant in the native chromosomal location (OG1RFΔ*liaR*Δ*c-dak*::*c-dak*). Of note, restoration of the gene resulted in a change in the last C-terminal amino acid (E558G), but this did not affect the phenotype. The complemented strain OG1RFΔ*liaR*Δ*c-dak*::*c-dak* displayed a normal growth phenotype and reverted the ceftriaxone MIC from >256 μg/mL to 12 μg/mL (Fig. 1, Table 1, **and** Table 2).

Changes in DAK result in specific alterations of the cell envelope ultrastructure.

Prior studies have reported changes in the cell envelope in DAP-R *E. faecalis* (Arias *et al.*, 2011). Using transmission electron microscopy (TEM), we evaluated the cell envelope structure of the DAP adapted mutants S613TMΔ$liaR_{yvcR219dak84asa1}$ and OG1RFΔ$liaR_{yxdK202dak371ace}$; and the mutants OG1RFΔ*yxdJ* and OG1RFΔ*liaR*Δ*c-dak*. In both OG1RFΔ$liaR_{yxdK202dak371ace}$ and OG1RFΔ*liaR*Δ*c-dak*, we observed cells with multiple septal events in which the orientation of the division plane was altered (Fig. 2, Supplemental Fig. 3). There was an increase in the thickness of the cellular envelope at the septal site, with cells displaying multiple protrusions of electron dense material from the cell surface. Complementation with the wild type *dak* allele restored the cell envelope structure in both OG1RFΔ$liaR_{yxdK202dak371ace}$ and OG1RFΔ*liaR*Δ*c-dak*. To investigate if the changes in cell envelope structure varied with growth phase, we compared OG1RFΔ*liaR* and OG1RFΔ*liaR*Δ*c-dak* at 8, 16 and 24 hours (Supplemental Fig. 4). The morphologic changes noted in OG1RFΔ*liaR*Δ*c-dak* were most prominent in late-exponential phase growth at 8 hours and less so at stationary phase (24 hours). Overall cell wall thickness of both OG1RFΔ$liaR_{yxdK202dak371ace}$ and OG1RFΔ*liaR*Δ*c-dak* was increased from the parent strain OG1RFΔ*liaR* at 16 hours, but this difference was statistically significant only for OG1RFΔ$liaR_{yxdK202dak371ace}$ ($p<0.01$) (Supplemental Fig. 5A). The phenotype observed in the DAP-R derivative of S613TMΔ*liaR* was less severe, without significant alterations of cell septum placement or cell wall thickness. This finding was supported by the lack of

major ultrastructural changes observed in OG1RFΔ*yxdJ*, suggesting that the C-terminal portion of DAK plays an important role in cell division homeostasis.

LiaR independent DAP-R is associated with alterations in membrane fluidity.

Resistance to DAP has been postulated to occur via multiple mechanisms, including alteration of cell surface charge (electrostatic repulsion) and variations in the content and architecture of the bacterial membrane, preventing DAP from reaching critical targets such as the division septum (diversion) (Tran *et al.*, 2015). To rule out a repulsion-mediated mechanism of resistance, we performed a global assessment of cell surface charge using a poly-L-lysine assay and found no significant differences in cell surface charge between strain pairs (Supplemental Fig. 5B).

In *E. faecalis*, a distinct redistribution of membrane phospholipid microdomains has been observed as a major mediator of DAP resistance via the LiaFSR system (Tran *et al.*, 2013). Thus, we sought to determine whether the observed mutations resulted in a similar alteration of the localization of membrane lipids. Using fluorescent microscopy with NAO, we were unable to detect any changes in the distribution of anionic phospholipid microdomains in either of the DAP adapted strains (Fig. 3A, Supplemental Figs. 6 **and** 7). Further, there was no decrease in the binding of BODIPY-DAP in the DAP resistant mutants as compared to their sensitive parental strains (Fig. 3B). In fact, OG1RFΔ$liaR_{yxdK202dak371ace}$ bound more DAP than the sensitive OG1RFΔ*liaR*, again implying that resistance is not mediated by repulsion of the antibiotic from the surface. Our data suggest that the mechanism of DAP-R mediated by changes in YxdJK and DAK appears to be distinct from that triggered by the LiaFSR system in *E. faecalis*.

DAP induced changes in membrane fluidity have recently been implicated in the antimicrobial action of the drug (Müller *et al.*, 2016), with sequestration of fluid membrane lipids observed in *B. subtilis* treated with DAP, as compared to untreated cells. The membrane dye laurdan possesses a variable emission spectrum responsive to lipid order, allowing spectroscopic measurement of membrane fluidity. Since it does not appear that LiaR-independent mutations divert DAP from its site of action (as previously shown (Tran *et al.*, 2013)), we postulated that they would interfere with membrane fluidity and potentially protect the cells against the antibiotic attack. In wild type OG1RF, we observed the characteristic shift towards a more rigid membrane after the addition of DAP at 10X the MIC and a more fluid membrane on incubation with ethanol (Fig. 4A). Interestingly, at lower DAP concentrations, we did not see a significant shift in rigidity in the DAP sensitive mutants OG1RFΔ*liaR* (DAP MIC 0.047 μg/mL) and OG1RFΔ$liaR_{yxdK202dak371ace}$Δ*yxdJ* (DAP MIC 0.094 μg/mL), despite the DAP concentration being ten times the MIC of the strain (Supplemental Fig. 8). Rigidity was induced in these strains at higher concentrations of DAP (200x MIC), thus the changes in rigidity did not appear to be due to the envelope stress response, and correlated with DAP concentration, but not strain MIC. Deletion of *liaR* did not alter baseline membrane fluidity (Fig. 4B). In OG1RFΔ$liaR_{yxdK202dak371ace}$ baseline membrane rigidity in log phase growth was significantly increased as compared to either OG1RF or OG1RFΔ*liaR*, and the membrane was more resistant to the induction of fluidity on addition of ethanol (Fig. 4C). This effect appears to be due to the changes in DAK, as

complementation of the wild type *dak* allele, but not inactivation of the YxdJK system, restored membrane fluidity to wild type levels (Fig. 4D-F). Once the cells reached stationary phase there was no significant difference in baseline rigidity (Supplemental Fig. 9). These findings suggest an altered membrane environment during active cell growth facilitates DAP resistance, and that alterations of membrane fluidity are necessary, but not sufficient, for the DAP resistance phenotype in *E. faecalis* OG1RF lacking *liaR*.

Discussion

We have previously shown that the LiaFSR system is crucial for development of antimicrobial peptide resistance in both *E. faecalis* and *E. faecium* (Panesso *et al.*, 2015; Reyes *et al.*, 2015). It has been proposed that this system could be targeted as a novel antimicrobial approach against these MDR organisms (anti-adaptation antibiotics). With that rationale, it becomes crucial to determine if resistance can develop in the absence of a functional LiaFSR system. Here, we demonstrate that DAP-R is able to arise independently of the presence of LiaR (the response regulator of the system), but with significant costs in cell fitness. More importantly, the LiaR-independent daptomycin resistance phenotype uncovered previously unknown genetic pathways leading to resistance to DAP and other cell envelope-targeting antimicrobials. In this work, we identified the TCS YxdJK (previously associated only with BAC resistance in *E. faecalis*) and a fatty acid metabolism enzyme harboring a DAK domain in association with DAP-R. The fact that mutations in genes encoding these proteins arose independently in two different strain backgrounds of *E. faecalis* lacking LiaR supports the concept that the cell membrane stress response network in enterococci is multi-layered as previously described in *B. subtilis* (Radeck *et al.*, 2016).

The YxdJK stress response system is known to regulate two ABC transporters in *Enterococcus faecalis*, one involved in signaling (YvcRS) and the other as the effector of the BAC resistance phenotype (YxdLM) (Gebhard *et al.*, 2014). These BceAB-type two component systems are conserved across the Firmicutes, with the YxdJK system present in *E. faecium* and *B. subtilis*, among others (Gebhard, 2012). We demonstrate that deletion of the response regulator YxdJ, responsible for activation of the ABC transporters, is sufficient to revert the resistant phenotype of OG1RFΔ$liaR_{yxdK202dak371ace}$. It is interesting to note that deletion of YxdJ in a background with a functional LiaFSR system leads to a 4-fold reduction in DAP MIC, suggesting an independent role of YxdJK in membrane homeostasis. Prior studies examining the cell wall response in *E. faecalis* OG1RF and JH2–2 showed that YxdJK was induced in response to BAC, mersacidin and cefalotin, but not ampicillin, nisin, gallidermin, vancomycin or teicoplanin (Abranches *et al.*, 2013; Gebhard *et al.*, 2014). We observed a similar phenomenon, with MIC shifts in BAC, CRO and DAP, but not ampicillin or vancomycin. This phenotype suggests that generalized responses to membrane induced stress, such as interference with lipid II or changes in cell wall homeostasis, are not the stimulus for YxdJK signaling. Instead, the system seems to sense antimicrobial compounds directly. The BceAB-type ABC transporters possess an extracellular domain postulated to interact with target molecules, a hypothesis supported by experiments in which extracellular domain swapping between transporters can alter substrate affinity (Gebhard, 2012). There is some evidence *in vitro* supporting a direct interaction between the permease subunit of the ABC transporter (YvcR homologue) and BAC in *B. subtilis* (Dintner *et al.*, 2014).

Elucidating the mechanism of antibiotic sensing and the specific downstream effects that bring about resistance is the basis of our future studies.

The DAK domain enzyme is conserved across the Firmicutes, with homology to the ATP-dependent dihyroxyacetone kinases of the glycolytic pathway (Siebold *et al.*, 2003). They possess two functional domains, the L-domain involved in ATP binding and the K-domain implicated in substrate phosphorylation, and have been demonstrated to mediate incorporation of exogenous fatty acids into the bacterial phospholipid synthesis pathway in *S. aureus* (Erni *et al.*, 2006; Parsons *et al.*, 2014). The presence of mutations at both a conserved serine residue in the ATP binding pocket and a premature stop codon disrupting the predicted EDD fold in the K-domain point to a decrease of enzyme activity in the DAP adapted strains. Indeed, a similar disruption of the C-terminal domain of DAK in *S. aureus* was found to impair activity of the antimicrobial peptide dermcidin and decrease membrane cardiolipin levels (Li *et al.*, 2009). Bacteria lacking DAK would be unable to utilize extracellular fatty acids, and would be dependent on the endogenous fatty acid synthesis pathway for membrane lipid biogenesis. This diversion of cellular metabolism into lipid biosynthesis may contribute to the DAK mutants' impaired growth phenotype. Loss of the C-terminal domain of DAK in OG1RF was associated with a significant increase in membrane rigidity as compared to strains with a wild type DAK allele. This shift in rigidity alone did not increase the DAP MICs of DAK mutants, but was required for changes in the YxdJK system to confer a fully DAP-R phenotype. In addition to DAP, these changes to the membrane may also affect other integral membrane or membrane associated proteins, such as those involved in cell division, and may also explain why these cells display a growth defect. The specific effects of the loss of DAK activity on membrane lipid composition are not clear.

A unique aspect of our observations of the C-terminal deletion of DAK was the unexpected effect on cell morphology. The fact that the predicted ATP-binding mutation did not show altered septal genesis suggests that either the enzymatic activity is only partially impaired, or that the C-terminal end of DAK is important for septal synthesis. From published data, it does not seem that loss of FakA, the DAK homologue in *S. aureus*, leads to impaired growth or an alteration of cellular morphology (Li *et al.*, 2009; Bose *et al.*, 2014; Parsons *et al.*, 2014). Conversely, screens for essential genes in *Streptococcus pneumoniae* (Zalacain *et al.*, 2003; Opijnen and Camilli, 2012) and our unsuccessful attempts to make a full in frame deletion in *E. faecalis* OG1RFΔ*liaR*, point to the N-terminal domain of the DAK protein as possessing an essential function in these bacteria. Further, the addition of exogenous fatty acids to growth media has been shown to confer protection against membrane stressors to *E. faecalis*, even those which lack LiaR (Saito *et al.*, 2014; Harp *et al.*, 2016). The mechanism of this protective effect is unknown, but may relate to changes in membrane composition. Given that membrane topology is important for correct localization of the division septum (Strahl and Errington, 2017) and metabolism and cell division are closely intertwined (Sperber and Herman, 2017), it is tempting to hypothesize that DAK mediated perturbation of membrane lipid composition impairs the bacteria's ability to define the division point of the cell, with marked effects on bacterial morphogenesis.

In summary, we show that DAP-R in *E. faecalis* may arise independently of the LiaFSR system, and identify the YxdJK signaling network as a cell envelope defense against multiple classes of clinically relevant antimicrobials. This resistance phenotype comes with a fitness cost, and our experiments suggest that changes in the DAK enzyme are responsible for the alterations of growth, cell envelope morphology and membrane fluidity seen in the *E. faecalis* mutants. Our findings underscore the robust nature of the enterococcal stress response and the identification of new pathways may provide important insights into disarming a challenging clinical pathogen.

Experimental Procedures

Bacterial strains, plasmids and growth conditions.

The bacterial strains and plasmids used in this work are listed in Table S1. We targeted two strains with previously generated non-polar deletions of *liaR* for mutagenesis, ***i)*** *E. faecalis* S613F$_{\Delta liaF177gdpD170cls61}$ (S613TMΔ*liaR*, DAP MIC 0.094 μg/mL) is a fusidic acid resistant derivative of clinical strain *E. faecalis* S613 containing three alleles associated with DAP-R (*liaF*, *cls* and *gdpD*) and a non-polar deletion of *liaR*, and ***ii)*** OG1RFΔ*liaR* (DAP MIC 0.047 μg/mL) is a derivative of *E. faecalis* OG1RF (Reyes *et al.*, 2015). Enterococcal strains were grown on Brain Heart Infusion Agar (BHI, Becton Dickinson) or in broth at 37˚ C with gentle agitation. The DAP adapted strain derivatives of S613TMΔ*liaR* and OG1RFΔ*liaR* were grown on BHI agar with DAP at 4 μg/mL and supplemented with 50 mg/L calcium chloride. *E. coli* strains EC1000 and TG-1 were grown on Luria-Bertani (LB) agar or in broth at 37˚ C with 25 μg/mL gentamicin added for propagation of pHOU1 or pAT392 containing constructs, respectively. Minimum inhibitory concentrations for each antibiotic were performed via Etest (bioMerieux) according to the manufacturer's instructions. Briefly, 0.5 McFarland standards for respective strains were prepared and inoculated onto Muller-Hinton agar plates (Oxoid). Strips were placed on the agar surface after absorption of inoculum, plates were placed at 37˚C and MICs were read after 24 hours of incubation. Slower growing mutants with *dak* mutations were read at 36 to 48 hours to allow a discernable lawn to develop.

In vitro *adaptation to daptomycin (DAP) of strains lacking liaR*.

S613TMΔ*liaR* and OG1RFΔ*liaR* were grown overnight on BHI agar from glycerol stocks and single colonies were inoculated into 10 mL of Muller-Hinton II broth supplemented with 50 mg/L of calcium chloride (MHC). DAP was added at 0.5x and 1x the MIC for each strain. The population with growth (as assessed by turbidity on visual inspection) at the highest DAP concentration was diluted 1:100 in fresh MHC media daily. Population MIC to DAP was determined by E-test (bioMerieux) on MH agar every other day, and this value was used to adjust the DAP concentration. Serial passage was continued until DAP-R colonies were obtained. DAP-R was defined as an increase in the MIC above 4 μg/mL (former CLSI breakpoint). Colonies growing inside the ellipse delineating the 4 μg/mL cutoff were picked and streaked on MHC agar supplemented with 4 μg/mL DAP and 50 mg/L $CaCl_2$ to isolate single colonies. The phenotype of purified colonies was verified by repeat DAP MIC determination via E-test.

Determination of stability and fitness.

Stability of the resistance phenotype for each strain was evaluated by DAP MIC determination after seven days of passage in antibiotic free media (BHI broth). Fitness of each strain was tested by comparing the growth curve of the DAP-R derivative strains to their DAP-S parents. Briefly, overnight cultures with BHI alone (parent strains) or BHI supplemented with 50 mg/L of $CaCl_2$ and 4 μg/mL DAP (derivative strains), were washed with fresh BHI media to remove antibiotics and used to prepare a 0.5 McFarland standard. This inoculum was diluted 1:100 into 96 well plates with a final volume of 200 μL per well in fresh BHI or MH media (without antibiotics) to yield approximately 5×10^5 CFU/mL. Two blank wells on each row were used for background correction. The optical density (OD) at 600 nm was measured at inoculation and every 15 minutes with shaking for 24 hours, using a Synergy H1 spectrophotometer (BioTek). Every third reading was plotted for ease of visualization. Data sets for each growth curve were analyzed by logistic regression using the R package Growthcurver (Sprouffske and Wagner, 2016). Colony counts were performed on a single run with each strain to verify that OD reading correlated with viable bacterial colony forming units.

Whole genome sequencing (WGS) and mutational analysis.

WGS of both isolates was carried out on a MiSeq (Illumina). Briefly, genomic DNA was isolated using the DNeasy Blood & Tissue kit (Qiagen) after lysozyme treatment. DNA libraries were prepared using the Nextera XT DNA Sample Preparation kit and sequenced with 150 bp paired-end reads. De novo assembly for each genome was done using CLCGenomics Workbench version 8.0.1 (CLCBio). The reads were trimmed (phred score ≥ 30), removing adapter sequences, and discarding those reads with length lower than 50 nucleotides. Single nucleotide polymorphism (SNP) calling was made by aligning the contigs from the assembly of the DAP-R derivative strains using the corresponding parent strains S613 and OG1RF, which were previously sequenced (Bourgogne *et al.*, 2008; Arias *et al.*, 2011), with BWA6 (Li and Durbin, 2009). The variant calling was made with Samtools and Bfctools (Li, 2011). The annotation of the SNPs was made with the SNPeff program (Cingolani *et al.*, 2012). The SNPs that were located on or upstream of coding regions were filtered for analysis and confirmed by Sanger sequencing.

Cloning and genetic manipulation of strains.

To investigate the contributions of genes identified via WGS, we constructed an isogeneic, non-polar deletion of *yxdJ* (the response regulator of the *yxdJK* system) by removing the sequence from the start codon to the stop codon of the open reading frame in both the OG1RF and OG1RFΔ$liaR_{yxdK202dak371ace}$ backgrounds. A deletion of the C-terminal end of DAK (Δ*c-dak*, removing the sequence encoding codon 371 to the 3' end of the gene) was constructed in OG1RF. All mutants were made using the *pheS** counterselection system, as previously described (Kristich *et al.*, 2007; Panesso *et al.*, 2011). Strains and primers used are listed in Table S1 and Table S2, respectively. Briefly, approximately 800 bp sequences flanking the regions of interest were amplified by PCR, cloned into pHOU1 (a shuttle vector that confers gentamicin resistance) using BamHI and EcoRI and propagated in *E. coli* EC1000 to generate the plasmids pHOU1::Δ*yxdJ* and pHOU1::Δ*c-dak*. After sequencing

each construct to verify integrity of the crossover region, plasmids were electroporated into *E. faecalis* CK111, then transferred by conjugation to the recipient strain OG1RF (for Δ*yxdJ*) or OG1RFΔ*liaR* (for Δ*c-dak*). Recipients were screened on BHI agar with 150 μg/mL of gentamicin, 25 μg/mL of fusidic acid and 125 μg/mL X-gal. The presence of the first crossover event was verified by PCR using primers in both flanks of the predicted insertion. Single colonies were suspended in 50 μL of normal saline and streaked on MM9YEG minimal media supplemented with 10mM *p*-chloro-phenylalanine to induce excision of the plasmid. White colonies, corresponding to bacteria in which pHOU1 have been excised, were screened for susceptibility to gentamicin and by PCR to assess for successful deletion of the target sequence. Mutants were confirmed with pulsed-field gel electrophoresis and sequencing of the crossover region to ensure that no additional changes were introduced.

Complementation in *trans* for the OG1RFΔ*yxdJ* mutant was carried out using the pAT392 shuttle vector which has a constitutive P2 promoter and the *aac(6')-aph(2")* gene allowing selection with gentamicin (Arthur *et al.*, 1994). Briefly, the region upstream of *yxdJ* containing the ribosomal binding site to the stop codon was amplified from OG1RF and cloned into pAT392 using the EcoRI and BamHI restriction sites. The resulting construct, pAT392::*yxdJ*, was transformed into *E. coli* TG-1, selected on LB agar plus 25 μg/mL gentamicin, screened by PCR and sequenced to verify the correct insert. OG1RFΔ*yxdJ* was made competent via growth in BHI supplemented with glycine and sucrose (Wirth *et al.*, 1986; Kristich *et al.*, 2007) and transformants were generated via electroporation with pAT392::*yxdJ* and selection on BHI plus 200 μg/mL gentamicin and screened by PCR to confirm presence of the insert. For the *dak* complementation in *cis*, the missing 3' end of the *dak* gene with flanking regions was amplified from OG1RF and cloned into pHOU1 using BamHI and EcoRI. Plasmid pHOU1 containing the intact *c-dak* gene for complementation was then electroporated into *E. faecalis* CK111 and mated to the OG1RFΔ$liaR_{yxdK202dak371ace}$ or OG1RFΔ*liaR*Δ*c-dak* strain as described above. After induction of plasmid excision, colonies with normal growth were screened by PCR for the full-length *dak* gene. Candidates were confirmed by sequencing of the crossover region.

Cell envelope structure determination by transmission electron microscopy (TEM).

Single colonies of each strain were inoculated into BHI and grown for 16 hours overnight. Cells were pelleted, washed three times in Millonig's phosphate buffer 0.1 M (13.85 g $NaH_2PO_4 \cdot H_2O$, 3.56 g NaOH in 1 L H_2O), and then fixed in 3% glutaraldehyde in Millonig's phosphate buffer. Samples were processed, embedded in paraffin and sectioned at the University of Texas Health Science Center Electron Microscopy Core. Imaging was carried out on a JEOL JEM 1200 EX Electron Microscope. Cell wall (CW) thickness was determined by measuring from the outer cell membrane to the edge of the cell wall at the pole and midpoint and averaging the two values. A minimum of 25 cells imaged at 50,000x were used to calculate mean CW thickness for each strain.

Determination of cell surface charge by poly-L-lysine binding.

Surface charge was assessed using fluorescein isothiocyanate (FITC) conjugated poly-L-lysine (Mukhopadhyay *et al.*, 2007). Cultures were grown overnight, washed three times

with 5mL of 5 mM HEPES pH 7.2 plus 5 mM glucose, and then resuspended in this same buffer to an absorbance value at 578 nm of 0.1. For each strain, 1 mL of the suspension was incubated with 10 μg of FITC-poly-L-lysine for 10 minutes. HEPES buffer plus FITC-poly-L-lysine without cells and cells alone were run in parallel for each strain, for total and background fluorescence, respectively. The cells were pelleted and 100 μL of the supernatant was placed in a light protected 96-well plate and fluorescence intensity was measured on an Infinite M1000 fluorescent spectrophotometer (Tecan) in technical triplicate. Since poly-L-lysine is a positively charged molecule, the concentration remaining in the supernatant is proportional to the overall cell surface charge, and the fluorescent signal intensity was normalized to the total fluorescence of 10 μg/mL FITC-poly-L-lysine in HEPES alone. The assay was repeated three times for each strain on different days.

Membrane phospholipid distribution and BODIPY-DAP binding by fluorescence microscopy.

Visualization of membrane anionic phospholipids was performed with *N*-nonyl acridine orange (NAO), a membrane dye with preferential binding to anionic phospholipid (e.g., cardiolipin), as described previously (Tran *et al.*, 2013). Briefly, cells grown to exponential phase were incubated with 500 nM NAO in the dark at 37˚ C for 3.5 hours. After staining, cells were washed with normal saline and immobilized on a poly-L-lysine coated coverslip (Sigma-Aldrich). Fluorescent images were taken on an Olympus IX71 or Keyence BX-700 microscope using a Nikon PlanApo N 100x objective, with a FITC filter set (excitation 490 nm, emission 528 nm).

Binding of BODIPY-FL labeled DAP (BODIPY-DAP, Cubist Pharmaceuticals) to cells *in vitro* and *in vivo*, was assessed as described previously (Tran *et al.*, 2013). Bacteria were grown to exponential phase in LB media supplemented with 50 mg/L of $CaCl_2$ at 37˚ C. BODIPY-DAP was then added at 4 μg/mL and 64 μg/mL and incubated for 10 minutes protected from light. Cells were washed three times in LB to remove unbound antibiotic, then immobilized on a poly-L-lysine coated coverslip. Cells were imaged using an Olympus IX71 or Keyence BX-700 microscope with a Nikon PlanApo N 100x objective and FITC filter set. Image processing was done using the Keyence software package and Adobe Photoshop CS5.

Membrane fluidity analysis by in vivo Laurdan generalized polarization spectroscopy.

Laurdan, 6-dodecanoyl-2-dimethylaminonaphthalene, is a membrane dye whose emission wavelength is responsive to changes in membrane phospholipid polarity, and, thus, alterations of membrane fluidity (Sanchez *et al.*, 2007). Laurdan generalized polarization (GP) spectroscopy was carried out according to a previously published protocol (Scheinpflug *et al.*, 2017), with the following modifications. Overnight cultures were inoculated into BHI supplemented with 0.1% glucose and grown at 37˚ C until an OD_{600} of 0.5 to 0.6, or 17 to 24 hours for stationary phase observations. A total of 1.9 mL of this culture was transferred to a 2 mL microcentrifuge tube and Laurdan (Molecular Probes, Thermo Fisher) was added to a final concentration of 10 μM, then incubated in a light protected box with shaking at 37˚ C for 10 minutes. The sample was then washed 4 times in 1 mL prewarmed (37˚ C) phosphate buffered saline (PBS) supplemented with 0.1% glucose

and 50 mg/L $CaCl_2$. After the final wash the sample was suspended in 1.9 mL of the PBS/glucose/calcium solution, and 4 technical replicates of 150 μL for each condition (untreated, DAP and ethanol) were placed into a light protected microtiter plate (Costar). An aliquot of 500 μL was taken from each sample, spun to pellet cells and two 150 μL aliquots of the supernatant were used to control for background fluorescence of Laurdan and Laurdan plus DAP. Baseline fluorescence intensity was measured with excitation at 350 nm and emission at 435 nm and 500 nm for five minutes at 37˚ C on a Synergy H1 spectrophotometer (BioTek) to allow equilibration of the cells. Cells were then treated with DAP at 10x the strain MIC, without antibiotics, or in the presence of 10% ethanol as a membrane fluidizer for 10 minutes, with measurements taken each minute as above. The Laurdan GP index was calculated with the formula $(I_{435}-I_{500})/(I_{435}+I_{500})$, where I is the fluorescent intensity at the specified wavelength. Experiments were run in duplicate on separate days.

Statistical analysis.

Differences in cell surface charge and cell wall thickness between strain pairs was compared by two way *t*-test using Prism 7.0 (GraphPad). For membrane fluidity, differences in mean Laurdan GP were assessed by 2-way ANOVA with correction using Dunnett's multiple comparisons test, using OG1RF as the control strain for each comparison. A difference in the mean value between samples was considered significant for *p*-values <0.05.

Accession Numbers.

Sequence data for the DAP-R strains was deposited with the National Center for Biotechnology Information (NCBI) GenBank, accession numbers NJIM00000000 (S613TMΔ$liaR_{yvcR219dak84asa1}$) and NJIN00000000 (OG1RFΔ$liaR_{yxdK202dak371ace}$).

Supplementary Material

Refer to Web version on PubMed Central for supplementary material.

Acknowledgements

Portions of this work were presented at ICAAC 2015, IDWeek 2015 and ASM 2017. Funding was provided by the National Institutes of Health, National Institute of Allergy and Infectious Diseases grants K08 AI135093 to WRM, K24-AI121296 and R01-AI134637 to CAA, R01AI080714 to YS and K08-AI113317 to TT. The funders had no role in study design, data collection or data interpretation. WRM has received grants, consulting fees and/or honoraria from Achaogen, Shionogi and Merck. TT has received grants from Merck. CAA has received grants from Merck and MeMed Diagnostics. All other authors have no reported conflicts.

References

Abranches J, Tijerina P, Avilés-Reyes A, Gaca AO, Kajfasz JK, and Lemos JA (2013) The Cell Wall-Targeting Antibiotic Stimulon of Enterococcus faecalis. PLoS One 8.

Arias CA, and Murray BE (2012) The rise of the Enterococcus: beyond vancomycin resistance. Nat Rev Microbiol 10: 266–78. [PubMed: 22421879]

Arias CA, Panesso D, McGrath DM, Qin X, Mojica MF, Miller C, et al. (2011) Genetic basis for in vivo daptomycin resistance in enterococci. N Engl J Med 365: 892–900. [PubMed: 21899450]

Arthur M, Depardieu F, Snaith HA, Reynolds PE, and Courvalin P (1994) Contribution of vanY D,D-carboxypeptidase to glycopeptide resistance in Enterococcus faecalis by hydrolysis of peptidoglycan precursors. Antimicrob Agents Chemother 38: 1899–1903. [PubMed: 7810996]

Bose JL, Daly SM, Hall PR, and Bayles KW (2014) Identification of the Staphylococcus aureus vfrAB operon, a novel virulence factor regulatory locus. Infect Immun 82: 1813–1822. [PubMed: 24549328]

Bourgogne A, Garsin DA, Qin X, Singh KV, Sillanpaa J, Yerrapragada S, et al. (2008) Large scale variation in Enterococcus faecalis illustrated by the genome analysis of strain OG1RF. Genome Biol 9: R110. [PubMed: 18611278]

Cingolani P, Platts A, Wang LL, Coon M, Nguyen T, Wang L, et al. (2012) A program for annotating and predicting the effects of single nucleotide polymorphisms, SnpEff: SNPs in the genome of Drosophila melanogaster strain w1118; iso-2; iso-3. Fly (Austin) 6: 80–92. [PubMed: 22728672]

Diaz L, Tran TT, Munita JM, Miller WR, Rincon S, Carvajal LP, et al. (2014) Whole-genome analyses of Enterococcus faecium isolates with diverse daptomycin MICs. Antimicrob Agents Chemother 58: 4527–4534. [PubMed: 24867964]

Dintner S, Heermann R, Fang C, Jung K, and Gebhard S (2014) A sensory complex consisting of an ATP-binding cassette transporter and a two-component regulatory system controls bacitracin resistance in Bacillus subtilis. J Biol Chem 289: 27899–27910. [PubMed: 25118291]

Erni B, Siebold C, Christen S, Srinivas A, Oberholzer A, and Baumann U (2006) Small substrate, big surprise: Fold, function and phylogeny of dihydroxyacetone kinases. Cell Mol Life Sci 63: 890–900. [PubMed: 16505971]

Gebhard S (2012) ABC transporters of antimicrobial peptides in Firmicutes bacteria - phylogeny, function and regulation. Mol Microbiol 86: 1295–1317. [PubMed: 23106164]

Gebhard S, Fang C, Shaaly A, Leslie DJ, Weimar MR, Kalamorz F, et al. (2014) Identification and characterization of a bacitracin resistance network in Enterococcus faecalis. Antimicrob Agents Chemother 58: 1425–1433. [PubMed: 24342648]

Harp JR, Saito HE, Bourdon AK, Reyes J, Arias CA, Campagna SR, and Fozo EM (2016) Exogenous fatty acids protect Enterococcus faecalis from daptomycin induced membrane stress independent of the response regulator LiaR. Appl Environ Microbiol 82: AEM.00933–16.

Humphries RM, Kelesidis T, Tewhey R, Rose WE, Schork N, Nizet V, and Sakoulas G (2012) Genotypic and phenotypic evaluation of the evolution of high-level daptomycin nonsusceptibility in vancomycin-resistant Enterococcus faecium. Antimicrob Agents Chemother 56: 6051–6053. [PubMed: 22948885]

Kelley LA, Mezulis S, Yates CM, Wass MN, and Sternberg MJE (2015) The Phyre2 web portal for protein modeling, prediction and analysis. Nat Protoc 10: 845–858. [PubMed: 25950237]

Kristich CJ, Chandler JR, and Dunny GM (2007) Development of a host-genotype-independent counterselectable marker and a high-frequency conjugative delivery system and their use in genetic analysis of Enterococcus faecalis. Plasmid 57: 131–144. [PubMed: 16996131]

Li H (2011) A statistical framework for SNP calling, mutation discovery, association mapping and population genetical parameter estimation from sequencing data. Bioinformatics 27: 2987–2993. [PubMed: 21903627]

Li H, and Durbin R (2009) Fast and accurate short read alignment with Burrows-Wheeler transform. Bioinformatics 25: 1754–1760. [PubMed: 19451168]

Li M, Rigby K, Lai Y, Nair V, Peschel A, Schittek B, and Otto M (2009) Staphylococcus aureus mutant screen reveals interaction of the human antimicrobial peptide dermcidin with membrane phospholipids. Antimicrob Agents Chemother 53: 4200–4210. [PubMed: 19596877]

Manson JM, Keis S, Smith JMB, and Cook GM (2004) Acquired bacitracin resistance in Enterococcus faecalis is mediated by an ABC transporter and a novel regulatory protein, BcrR. Antimicrob Agents Chemother 48: 3743–3748. [PubMed: 15388429]

Miller C, Kong J, Tran TT, Arias CA, Saxer G, and Shamoo Y (2013) Adaptation of Enterococcus faecalis to daptomycin reveals an ordered progression to resistance. Antimicrob Agents Chemother 57: 5373–5383. [PubMed: 23959318]

Mukhopadhyay K, Whitmire W, Xiong YQ, Molden J, Jones T, Peschel A, et al. (2007) In vitro susceptibility of Staphylococcus aureus to thrombin-induced platelet microbicidal protein-1 (tPMP-1) is influenced by cell membrane phospholipid composition and asymmetry. Microbiology 153: 1187–1197. [PubMed: 17379728]

Müller A, Wenzel M, Strahl H, Grein F, Saaki TNV, Kohl B, et al. (2016) Daptomycin inhibits cell envelope synthesis by interfering with fluid membrane microdomains. Proc Natl Acad Sci U S A 113: E7077–E7086. [PubMed: 27791134]

Munita JM, Panesso D, Diaz L, Tran TT, Reyes J, Wanger A, et al. (2012) Correlation between mutations in liaFSR of Enterococcus faecium and MIC of daptomycin: Revisiting daptomycin breakpoints. Antimicrob Agents Chemother 56: 4354–4359. [PubMed: 22664970]

Munita JM, Tran TT, Diaz L, Panesso D, Reyes J, Murray BE, and Ariasa CA (2013) A liaf codon deletion abolishes daptomycin bactericidal activity against vancomycin-resistant Enterococcus faecalis. Antimicrob Agents Chemother 57: 2831–2833. [PubMed: 23507277]

Opijnen T. Van, and Camilli A (2012) A fine scale phenotype − genotype virulence map of a bacterial pathogen. Genome Res 22: 2541–2551. [PubMed: 22826510]

Palmer KL, Daniel A, Hardy C, Silverman J, and Gilmore MS (2011) Genetic basis for daptomycin resistance in enterococci. Antimicrob Agents Chemother 55: 3345–3356. [PubMed: 21502617]

Panesso D, Montealegre MC, Rincón S, Mojica MF, Rice LB, Singh KV, et al. (2011) The hylEfm gene in pHylEfm of Enterococcus faecium is not required in pathogenesis of murine peritonitis. BMC Microbiol 11: 20. [PubMed: 21266081]

Panesso D, Reyes J, Gaston E, Deal M, Londoño A, Nigo M, et al. (2015) Deletion of liaR Reverses Daptomycin Resistance in Enterococcus faecium Independent of the Genetic Background. Antimicrob Agents Chemother 59: AAC.01073–15.

Parsons JB, Broussard TC, Bose JL, Rosch JW, Jackson P, Subramanian C, and Rock CO (2014) Identification of a two-component fatty acid kinase responsible for host fatty acid incorporation by Staphylococcus aureus. Proc Natl Acad Sci U S A 111: 10532–7. [PubMed: 25002480]

Prieto AMG, Wijngaarden J, Braat JC, Rogers MRC, Majoor E, Brouwer EC, et al. (2017) The Two-Component System ChtRS Contributes to Chlorhexidine Tolerance in Enterococcus faecium. Antimicrob Agents Chemother 61: 1–9.

Radeck J, Gebhard S, Orchard PS, Kirchner M, Bauer S, Mascher T, and Fritz G (2016) Anatomy of the bacitracin resistance network in Bacillus subtilis. Mol Microbiol 100: 607–620. [PubMed: 26815905]

Reyes J, Panesso D, Tran TT, Mishra NN, Cruz MR, Munita JM, et al. (2015) A liaR deletion restores susceptibility to daptomycin and antimicrobial peptides in multidrug-resistant Enterococcus faecalis. J Infect Dis 211: 1317–1325. [PubMed: 25362197]

Saito HE, Harp JR, and Fozo EM (2014) Incorporation of exogenous fatty acids protects Enterococcus faecalis from membrane-damaging agents. Appl Environ Microbiol 80: 6527–6538. [PubMed: 25128342]

Sanchez SA, Tricerri MA, Gunther G, and Gratton E (2007) Laurdan Generalized Polarization: from cuvette to microscope. Mod Res Educ Top Microsc 2: 1007–1014.

Scheinpflug K, Krylova O, and Strahl H (2017) Measurement of Cell Membrane Fluidity by Laurdan GP: Fluorescence Spectroscopy and Microscopy. In Antibiotics: Methods and Protocols pp. 159–174.

Siebold C, Arnold I, Garcia-Alles LF, Baumann U, and Erni B (2003) Crystal Structure of the Citrobacter freundii Dihydroxyacetone Kinase Reveals an Eight-stranded alpha-Helical Barrel ATP-binding Domain. J Biol Chem 278: 48236–48244. [PubMed: 12966101]

Sperber AM, and Herman JK (2017) Metabolism shapes the cell. J Bacteriol 199: 1–14.

Sprouffske K, and Wagner A (2016) Growthcurver: An R package for obtaining interpretable metrics from microbial growth curves. BMC Bioinformatics 17: 17–20. [PubMed: 26729273]

Strahl H, and Errington J (2017) Bacterial Membranes : Structure, Domains, and Function 519–538.

Tran TT, Munita JM, and Arias CA (2015) Mechanisms of drug resistance: Daptomycin resistance. Ann N Y Acad Sci 1354: 32–53. [PubMed: 26495887]

Tran TT, Panesso D, Mishra NN, Mileykovskaya E, Guan Z, Munita JM, et al. (2013) Daptomycin-resistant Enterococcus faecalis diverts the antibiotic molecule from the division septum and remodels cell membrane phospholipids. MBio 4: 1–10.

Weiner LM, Webb AK, Limbago B, Dudeck M, Patel J, Kallen AJ, et al. (2016) Antimicrobial-Resistant Pathogens Associated With Healthcare-Associated Infections: Summary of Data

Reported to the National Healthcare Safety Network at the Centers for Disease Control and Prevention, 2011–2014. Infect Control Hosp Epidemiol 37: 1288–1301. [PubMed: 27573805]

Wirth R, An FY, and Clewell DB (1986) Highly efficient protoplast transformation system for Streptococcus faecalis and a new Escherichia coli-S. faecalis shuttle vector. J Bacteriol 165: 831–836. [PubMed: 3005240]

Zalacain M, Biswas S, Ingraham KA, Ambrad J, Bryant A, Chalker AF, et al. (2003) A global approach to identify novel broad-spectrum antibacterial targets among proteins of unknown function. J Mol Microbiol Biotechnol 6: 109–126. [PubMed: 15044829]

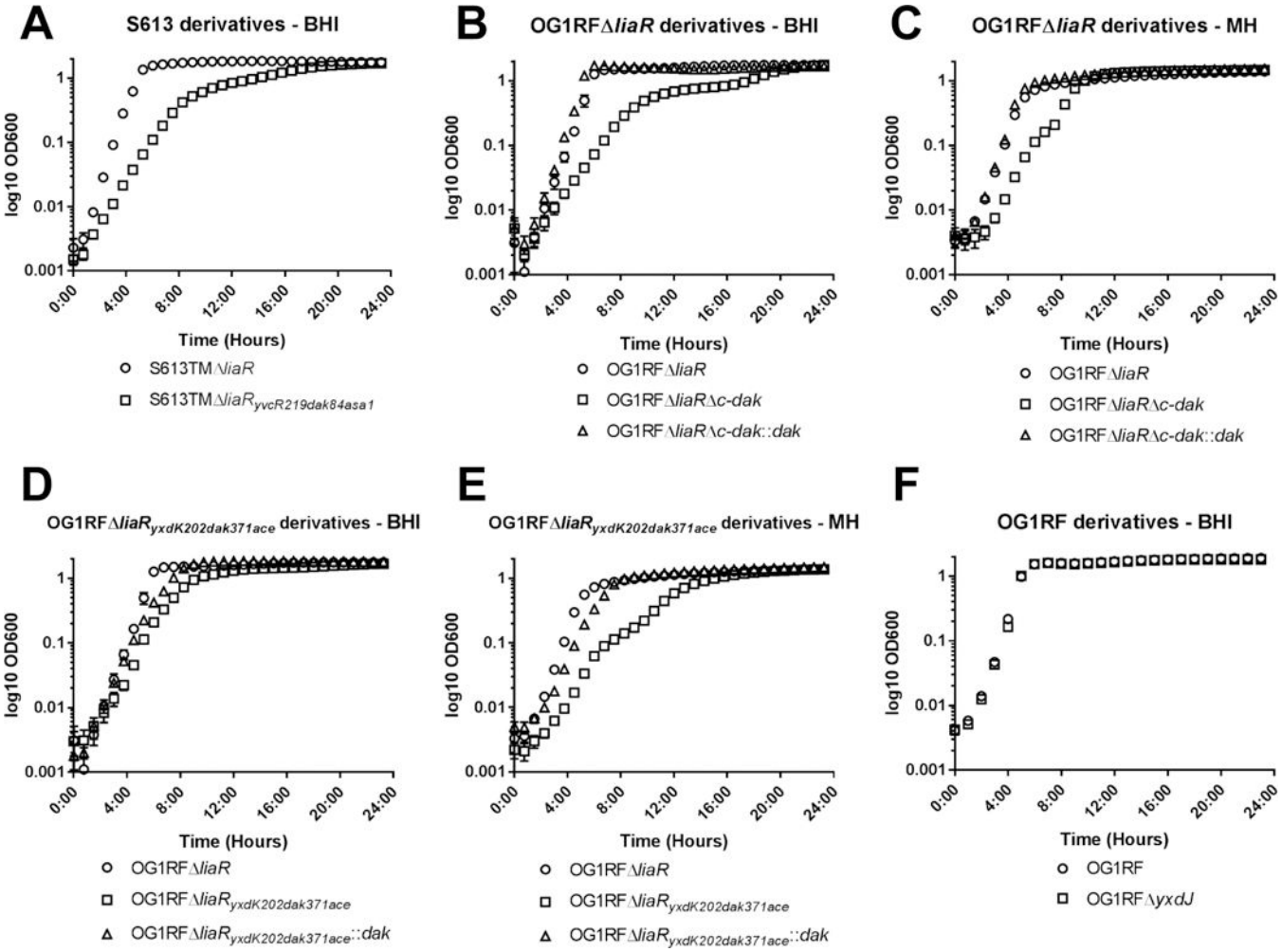

Figure 1. LiaR independent DAP-R is associated with impaired growth.

Growth curves in media without antibiotics for the (A) S613 background, (B and C) OG1RFΔ*liaR* background, (D and E) OG1RFΔ$liaR_{yxdK202dak371ace}$ background, and (F) wild type OG1RF background. Derivatives with mutations in *dak* showed alterations in growth (also see Table 2) independent of media, and reintroduction of the wild type *dak* allele complemented the growth phenotype. Error bars represent the standard error of the mean from three independent runs, n=10 measurements per strain. BHI, brain heart infusion; MH, Mueller Hinton.

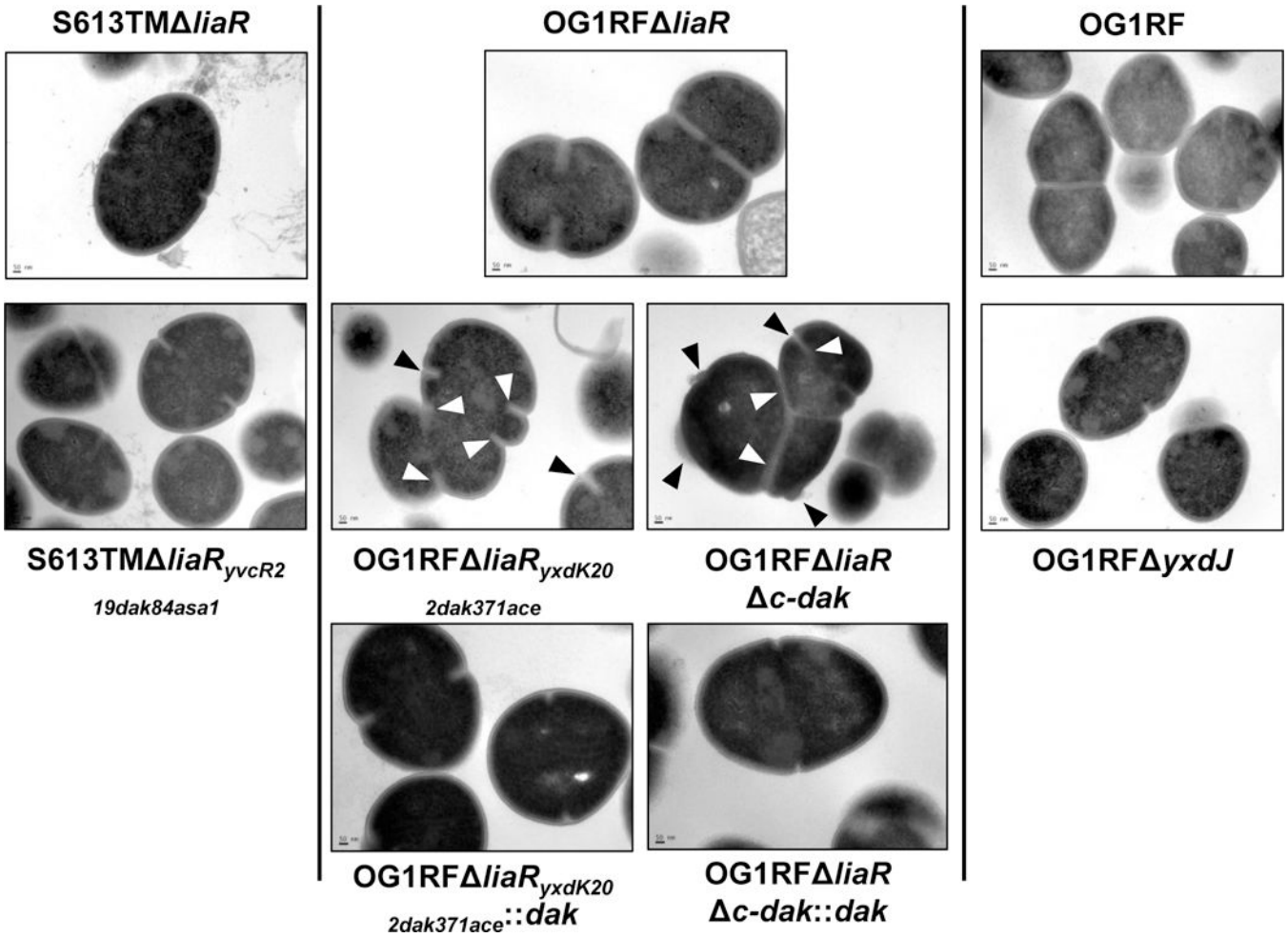

Figure 2. Loss of the C-terminal domain of DAK leads to altered cell morphology.

Transmission electron microscopy (TEM) of parent strains (top row), derivative strains (middle row), and complemented strains (bottom row) displaying changes in cell envelope structure. In OG1RFΔ*liaR* septa are positioned at the middle of the cell, with one septal event per cell. In OG1RFΔ$liaR_{yxdK202dak371ace}$, multiple septal events per cell can be seen (white arrows), with loss of the division plane orientation, resulting in distorted cells. Cell envelope at the site of division is thickened, with small burs or protrusions from the cell surface (black arrows). A similar phenotype can be observed in OG1RFΔ*liaR*Δ*c-dak*, suggesting this domain plays an important role in cell division. These changes were not seen when the full length *dak* gene was complemented back to its chromosomal location. S613TMΔ$liaR_{yvcR219dak84asa1}$ and OG1RFΔ*yxdJ* did not show structural changes. Scale bar for all images, 50 nm; Images are representative of over 25 different fields, wide field images are displayed in supplementary figure 3.

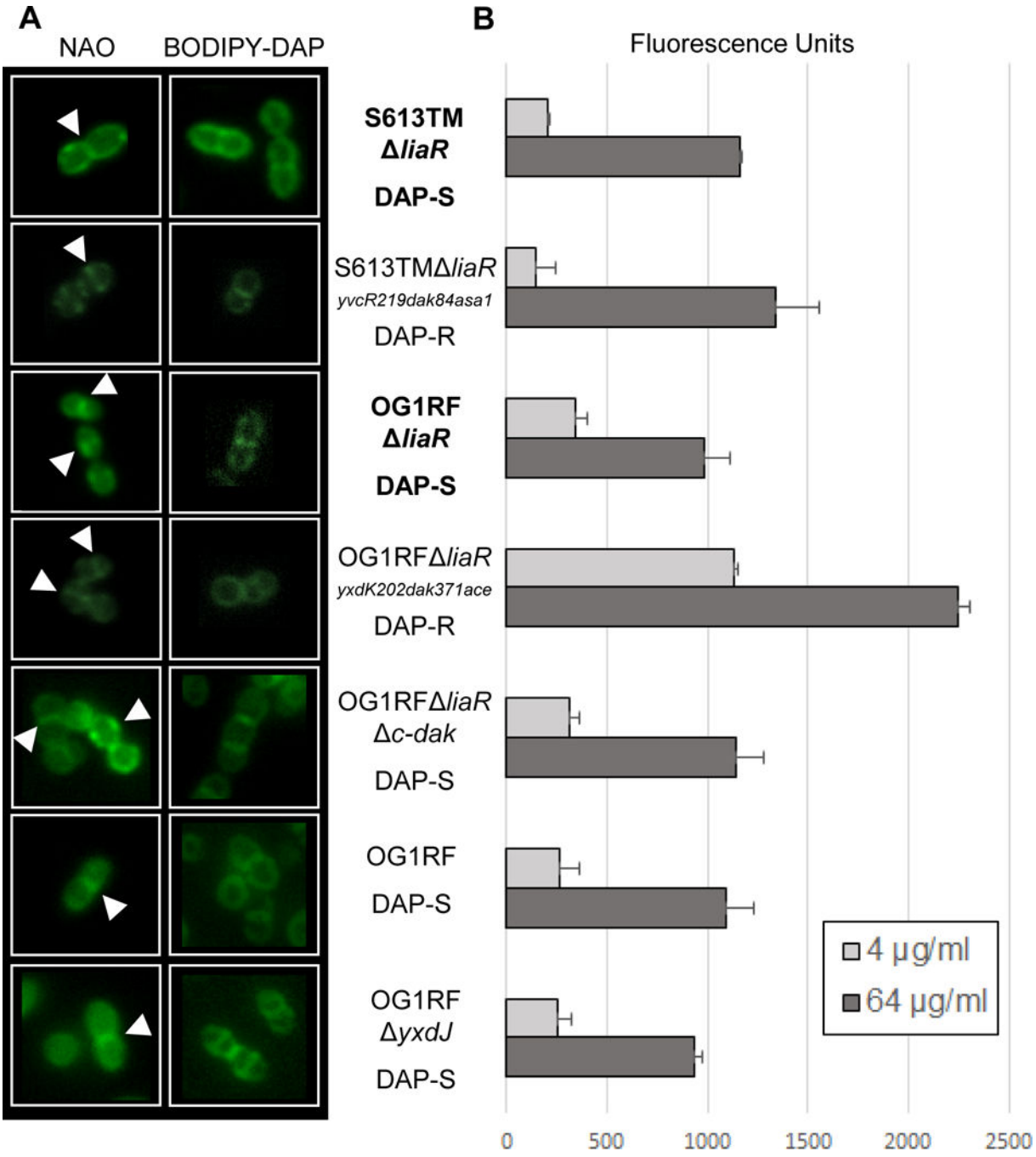

Figure 3. DAP-R independent of LiaR does not result in phospholipid microdomain redistribution or a reduction in DAP binding.

(A) *N*-nonyl acridine orange (NAO) and BODIPY-DAP staining of *E. faecalis* strains. NAO is a membrane dye that associates with anionic phospholipids, particularly cardiolipin. In all strains NAO and BODIPY-DAP can be seen localizing to the division septum (white arrows), without any areas of redistribution. (B) Quantitative BODIPY-DAP binding. Comparisons in binding were made between parental stains (bold) and derivatives. Increased DAP binding was seen in OG1RFΔ$liaR_{yxdK202dak371ace}$ at both 4 and 64 µg/mL as compared

to OG1RFΔ*liaR*. No significant changes were seen between the other strain pairs. Representative results of two independent runs performed on different days.

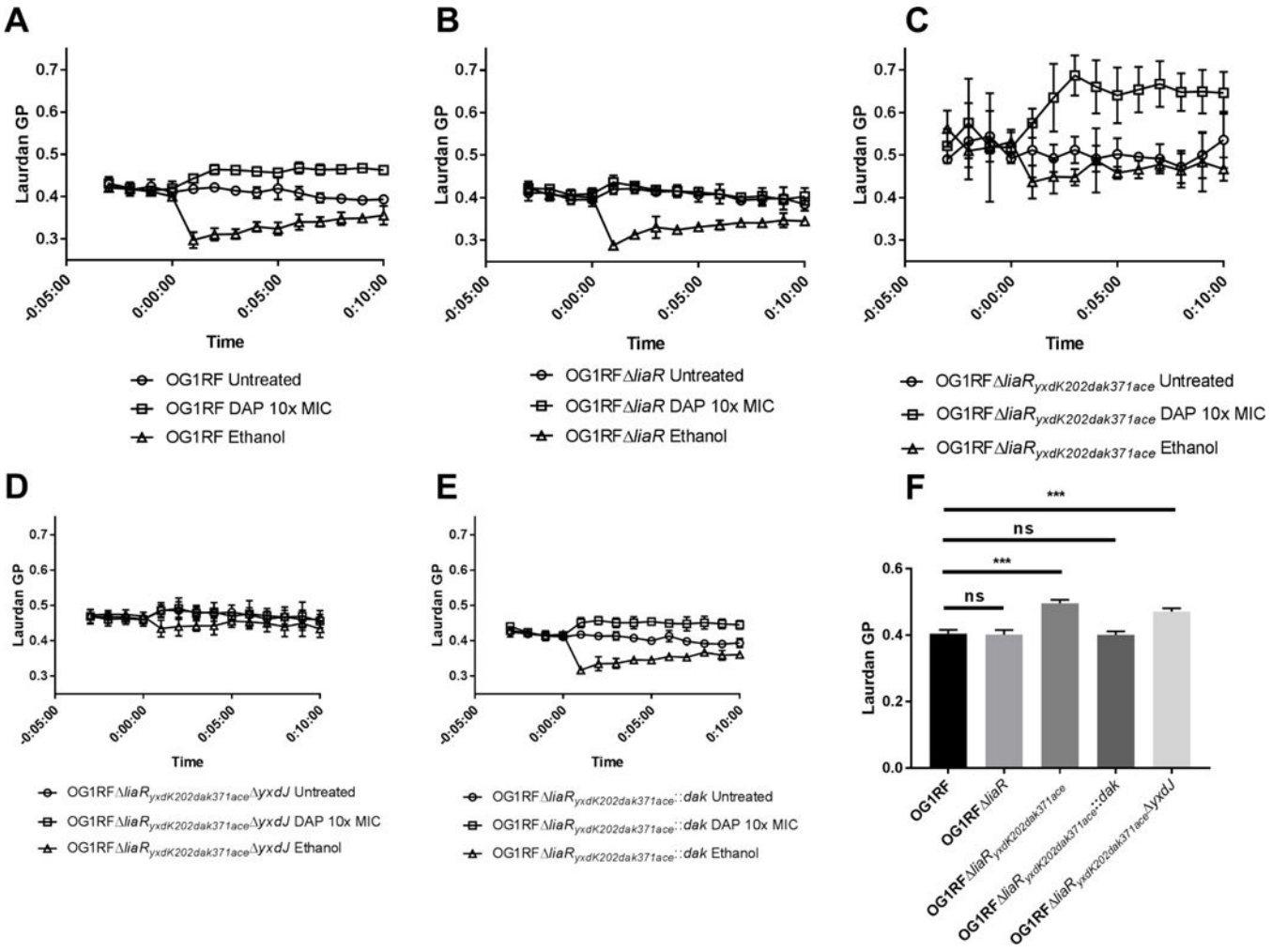

Figure 4. Mutations in DAK and *yxdJ* alter membrane fluidity.

Membrane fluidity was assayed using the fluorescent dye laurdan, whose emission spectrum shifts in response to the order of the lipid bilayer (higher numbers indicate increasing rigidity). Representative results are displayed as the mean and standard deviation of two independent experiments run in technical quadruplicate, with DAP or ethanol added at time=0. (A) and (B) show that baseline fluidity and fluidity after the addition of ethanol are similar for both OG1RF and OG1RFΔ*liaR*. (C) and (D) As compared to OG1RF wild type, mutants with changes in DAK had a significantly more rigid membrane at baseline, and were more resistant to the fluidity shift after addition of ethanol. (E) Complementation with the wild type *dak* allele restored membrane fluidity to wild type levels. (F) Comparison of mean baseline fluidity by two-way ANOVA with correction using Dunnett's multiple comparisons test, using OG1RF as the control strain for comparison. ***$p<0.001$; ns, non-significant. Representative results of two independent assays for each strain performed on different days.

Table 1.

Antimicrobial Minimum Inhibitory Concentrations of *E. faecalis* Strains.

Strain	DAP	BAC	CRO	AMP	VAN
S613	0.5	>256	>256	0.38	>256
S613TM	8	>256	>256	0.125	>256
S613TMΔ*liaR*	0.094	>256	>256	0.38	>256
S613TMΔ$liaR_{yvcR219dak84asa1}$	24	>256	>256	1	>256
OG1RF	1.5	64	32	0.5	2
OG1RFΔ*liaR*	0.047	4	16	0.5	2
OG1RFΔ$liaR_{yxdK202dak371ace}$	6	96	>256	1	3
OG1RFΔ$liaR_{yxdK202dak371ace}$Δ*yxdJ*	0.094	0.75	>256	3	1.5
OG1RFΔ$liaR_{yxdK202dak371ace}$Δ*yxdJ*/pAT392::*yxdJ*	3	>256	>256	0.38	1
OG1RFΔ$liaR_{yxdK202dak371ace}$::*dak*	2	128	>256	3	3
OG1RFΔ*yxdJ*	0.38	12	8	0.5	3
OG1RFΔ*yxdJ*/pAT392::*yxdJ*	2	64	48	1	3
OG1RFΔ*yxdJ*/pAT392	0.5	12	8	1	3
OG1RFΔ*liaR*Δ*c-dak*	0.064	1.5	>256	0.5	2
OG1RFΔ*liaR*Δ*c-dak*::*c-dak*	0.047	6	12	1.5	3

All values in μg/ml. DAP, daptomycin; BAC, bacitracin; CRO, ceftriaxone; AMP, ampicillin; VAN, vancomycin.

Table 2.

Growth Parameters for *E. faecalis* Strains.

	BHI		MH	
	Lag Time[†] ± SD	**Growth Rate[§] ± SD**	**Lag Time[†] ± SD**	**Growth Rate[§] ± SD**
OG1RFΔ*liaR*	76.2 ± 22	3.31 ± 0.58	83.7 ± 8	1.31 ± 0.03
OG1RFΔ*liaR*Δ*c-dak*	106.2 ± 42	0.77 ± 0.17	154.2 ± 9	0.88 ± 0.1
OG1RFΔ*liaR*Δ*c-dak*::*c-dak*	68.7 ± 25	4.70 ± 1.07	79.2 ± 9	1.49 ± 0.03
OG1RFΔ$liaR_{yxdK202dak371ace}$	80.7 ± 26	0.86 ± 0.07	158.7 ± 14	0.67 ± 0.04
OG1RFΔ$liaR_{yxdK202dak371ace}$::*dak*	73.2 ± 13	1.29 ± 0.05	86.7 ± 10	1.11 ± 0.04
S613TMΔ*liaR*	47.7 ± 8	1.84 ± 0.07	ND	ND
S613TMΔ$liaR_{yvcR219dak84asa1}$	73.2 ± 15	0.88 ± 0.02	ND	ND
OG1RF	58.2 ± 11	2.39 ± 0.06	ND	ND
OG1RFΔ*yxdJ*	62.7 ± 8	2.81 ± 0.22	ND	ND

[†]Minutes.

[§]Maximal rate of change, OD per hour.

BHI, brain heart infusion broth; MH, Mueller Hinton broth; ND, not done; SD, standard deviation.

Table 3.

Nonsynonymous Single Nucleotide Polymorphisms Identified by Whole Genome Sequencing in S613TMΔ*liaR*$_{yvcR219dak84asa1}$ and OG1RFΔ*liaR*$_{yxdK202dak371ace}$.

	S613TMΔ*liaR*$_{yvcR219dak84asa1}$				
Gene	**Locus tag (V583 genome)**	**Locus tag (OG1RF genome)**	**NT Change**	**AA change**	**Predicted function**
yvcR	EF2752	OG1RF_12114	2443262, T>G	D219A	ABC Transporter, ATP binding subunit
dak	EF3114	OG1RF_12374	2711659, A>G	S84P	DAK domain protein, fatty acid kinase
asa1	EF0485	-	377891, G>A 378128, A>C 378268, C>A 378269, A>C 378335, A>C	D1034N I1113L D1159E K1160Q N1182H	Cell surface adhesin and virulence factor
	OG1RFΔ*liaR*$_{yxdK202dak371ace}$				
Gene	**Locus tag (V583 genome)**	**Locus tag (OG1RF genome)**	**NT Change**	**AA change**	**Predicted function**
yxdK	EF0927	OG1RF_10654	689129, C>A	A202E	Sensor histidine kinase
dak	EF3114	OG1RF_12374	2512631 G>A	Q371*	DAK domain protein, fatty acid kinase
ace	EF1099	OG1RF_10878	918431, C>T 918448, A>G 918478, G>A	A462V S468G A478T	collagen adhesin, virulence factor

NT, nucleotide; AA, amino acid; ABC, ATP-Binding Cassette; DAK, Dihydroxyacetone kinase